# Surface tension of the most popular models of water by using the test-area simulation method

C. Vega[a)]
*Departamento de Química Física, Facultad de Ciencias Químicas, Universidad Complutense, 28040 Madrid, Spain*

E. de Miguel
*Departamento de Física Aplicada, Facultad de Ciencias Experimentales, Universidad de Huelva, 21071 Huelva, Spain*

(Received 22 December 2006; accepted 16 February 2007; published online 19 April 2007)

We consider the calculation of the surface tension from simulations of several models of water, such as the traditional TIP3P, SPC, SPC/E, and TIP4P models, and the new generation of TIP4P-like models including the TIP4P/Ew, TIP4P/Ice, and TIP4P/2005. We employ a thermodynamic route proposed by Gloor *et al.* [J. Chem. Phys. **123**, 134703 (2005)] to determine the surface tension that involves the estimate of the change in free energy associated with a small change in the interfacial area at constant volume. The values of the surface tension computed from this test-area method are found to be fully consistent with those obtained from the standard mechanical route, which is based on the evaluation of the components of the pressure tensor. We find that most models do not reproduce quantitatively the experimental values of the surface tension of water. The best description of the surface tension is given by those models that provide a better description of the vapor-liquid coexistence curve. The values of the surface tension for the SPC/E and TIP4P/Ew models are found to be in reasonably good agreement with the experimental values. From the present investigation, we conclude that the TIP4P/2005 model is able to accurately describe the surface tension of water over the whole range of temperatures from the triple point to the critical temperature. We also conclude that the test area is an appropriate methodological choice for the calculation of the surface tension not only for simple fluids, but also for complex molecular polar fluids, as is the case of water. © *2007 American Institute of Physics*. [DOI: 10.1063/1.2715577]

## I. INTRODUCTION

The pioneering work of Barker and Watts[1] and Rahman and Stillinger[2] started the area of computer simulation of water and thousands of papers have been devoted to the determination of the properties of this system by computer simulation ever since. The number of potential models of water proposed so far is huge[3,4] and some of them have become more popular in the field of water potentials. This is the case of the simple rigid nonpolarizable TIP3P,[5] TIP4P,[5] SPC,[6] SPC/E,[7] and TIP5P[8] models. These five model potentials are used in the overwhelming majority of simulations where water is present (for instance, in the field of computer simulation of biological molecules[4]). These potentials are computationally cheap, with a Lennard-Jones (LJ) site located on the oxygen atom, and partial positive charges located on the hydrogen atoms. The negative charge is located along the bisector of the H–O–H bond in the TIP4P model, whereas this charge is placed on the oxygen atom in the TIP3P, SPC, and SPC/E models. In the TIP5P model, the negative charges are located on the "lone pairs" electrons. The main differences between these model potentials lie in the location of the negative charge and in the set of properties that are fitted to obtain the potential parameters. There has been evidence over the last years that these models could be easily improved. In fact, slight changes in the values of the parameters and/or in the choice of properties to be fitted may result in an improved model potential for water.

Due to the increasing popularity of the Ewald sums to deal with long-range Coulombic forces, partly due to the advent of the efficient particle mesh Ewald[9] (PME) technique, this new generation of potential models has been specifically designed to be used with Ewald sums (or with any other technique that includes a proper treatment of the long-range interactions, as is the case of the reaction field). It is with this idea in mind that the TIP4P/Ew (Ref. 10) and TIP4P/2005 (Ref. 11) models have recently been proposed. These two models reproduce quite nicely one of the fingerprint properties of water: the maximum in density of water at room pressure. A new model, known as the TIP4P/Ice,[11] has also been proposed and has been found to reproduce the experimental melting temperature of water. The choice of the TIP4P geometry to improve current models of water is based on the fact that models with this geometry are found to provide a qualitatively correct description of the phase diagram of water, whereas the TIP3P, SPC, SPC/E, and TIP5P models fail in this regard.[12–15] Their melting points (with the exception of TIP5P) are too low,[16,17] and moreover, for TIP3P, SPC, SPC/E, and TIP5P ice II is more stable than ice $I_h$ at room pressure.[16] It seems clear that TIP4P/Ice, TIP4P/2005, and to a less extent TIP4P/Ew models are appropriate to

[a)]Electronic mail: cvega@quim.ucm.es

 

describe properties of the different solid phases of water, and of the fluid-solid and solid-solid equilibria of water. The good performance of these models is not limited to the solid phase but also to the vapor-liquid equilibria. Although the TIP4P/Ice model significantly overestimates the value of the critical temperature,[18,19] it has been found[18] that the TIP4P/Ew model yields a much better prediction of the vapor-liquid critical point than the traditional (SPC, TIP3P, and TIP5P) models. In addition, the TIP4P/2005 model has been shown to give a fairly good prediction of the vapor-liquid equilibria and critical properties of water.[18] The only traditional model with a similar (although slightly worse) performance is the SPC/E.[20,21] At this stage, one may assess that the TIP4P/2005 model seems to provide a good description of solid densities, phase diagrams, liquid properties, phase equilibria, and critical properties.

Once the global phase equilibria of practically all models of water is known it seems of interest to study the ability of the different models to predict interfacial properties, as is the case of the surface tension of the vapor-liquid interface. The determination of the surface tension of water by computer simulation has been the subject of several studies.[22–38] In the majority of these studies, a slab of liquid is placed in contact with vapor and the surface tension is computed from a mechanical route which requires the calculation of the pressure tensor.[39] A survey of the literature reveals that values of the surface tension from different authors differ in some cases considerably. One possible reason of the discrepancies is that reliable values of the surface tension (or any other interfacial property) are only obtained after considering sufficiently large systems and long simulation runs.[40] Secondly, the truncation of the potential is known to significantly affect the interfacial properties and different authors typically use different values of the cutoff distance.[41] Also there could be finite-size effects when the area of the interface is too small.

Here, we consider simulations of the vapor-liquid interface of different models of water and determine the surface tension from the test-area method recently proposed by Gloor *et al.*[42] The method relies on the computation of the surface tension from the change in free energy in the limit of an infinitesimal perturbation in the area of the interface at constant volume. It can be shown that the free-energy change associated with this perturbation can be expressed in terms of the average of the Boltzmann factor of the change in configurational energy resulting from the perturbation. The method bears some resemblance to the Widom test-particle method,[43–45] where the chemical potential follows from the evaluation of the average of the Boltzmann factor associated with the potential energy resulting from adding a ghost particle. In both cases, a normal simulation of the system is carried out, and a virtual move is performed periodically; this virtual move implies the addition of a particle in the Widom test-particle method, and the change in the area of the interface (at constant volume) in the test-area method. A similar free-energy perturbation approach has been considered for the calculation of the bulk pressure[46] or the components of the pressure tensor.[47–49] Gloor *et al.*[42] have shown that the test-area method can be used for simple systems (LJ or square wells) with results in full agreement with those obtained from the conventional virial route. They have also shown that the methodology can be used for molecular fluids such as the Gay Berne model.[42] We implement in this paper the test-area method to compute the surface tension of different models of water and the results are compared with those obtained from the virial route. In particular, we consider the traditional SPC, SPC/E, TIP3P, and TIP5P models, as well as the most recent TIP4P/Ice, TIP4P/2005, and TIP4P/Ew models of water. The purpose is twofold. On one hand we would like to show that the methodology of Gloor *et al.* can also be used for molecular fluids with long-range Coulombic forces. On the other hand, the computation of the surface tension from two independent routes may be of help considering the disparity between results available in the literature. According to our results, both routes to the calculation of the surface tension are found to be fully consistent. We also find that most models fail in describing the surface tension of water. The SPC/E and TIP4P/Ew models provide a reasonable description, whereas the TIP4P/2005 model yields values of the surface tension in quantitative agreement with experiments over the range of temperatures from the triple point to the critical temperature.

## II. METHODOLOGY

We consider in our simulations a slab of liquid consisting of $N=1024$ molecules of water placed in between two empty regions. The simulations are performed at constant temperature $T$ and volume $V$ in an orthorhombic simulation cell of dimensions $L_x \approx L_y \approx 30$ Å, and $L_z = 100$ Å. For a subcritical temperature, this setup is expected to stabilize two planar vapor-liquid interfaces perpendicular to the $z$ axis of the simulation cell. Molecular dynamics simulations are performed using GROMACS (version 3.3)[50] to generate the molecular trajectories using a time step of 1 fs. The temperature is kept constant by using a Nose-Hoover[51,52] thermostat with a relaxation time of 2 ps. The inhomogeneous system is first allowed to equilibrate over 300 ps, and running averages are then collected over an additional run of 1.5–2 ns depending on the thermodynamic conditions. The geometry of the water molecules is enforced using constraints.[53,54] This poses a problem when the molecular model of water includes massless interaction sites, as is the case of the TIP4P and TIP5P models. These are treated in a special way: the location of the molecule is calculated from the positions of the other sites and the force is redistributed on the other atoms.[54,55] The LJ part of the potential is truncated at 13 Å and a switching function is used between 12 and 13 Å. Ewald sums are used to deal with the electrostatic interactions. The real part of the Coulombic potential is truncated at 13 Å. The Fourier part of the Ewald sums are evaluated by using the PME method of Essmann *et al.*[9] The width of the mesh is set equal to 1 Å, and fourth-other interpolation is used.

The version of GROMACS used here yields the components of the pressure tensor, which in turn allow us to compute the surface tension $\gamma$. For a planar interface perpendicular to the $z$ axis, $\gamma$ is given by[39]

$$\gamma = \int_{-\infty}^{\infty} dz[p_N(z) - p_T(z)] = L_z[\bar{p}_N - \bar{p}_T], \tag{1}$$

where $p_N(z)$ and $p_T(z)$ are the normal and tangential (local) components of the pressure tensor at position $z$, respectively. For a planar interface, $p_N$ does not depend on $z$ and is equal to the vapor pressure, $p$; $\bar{p}_N$ and $\bar{p}_T$ in Eq. (1) are macroscopic components of the pressure tensor defined in terms of the volume average of their local components counterparts.[42] Considering that the setup of our simulations stabilizes two vapor-liquid interfaces, the working expression for the computation of the surface tension turns out to be

$$\gamma = \frac{L_z}{2}[\bar{p}_N - \bar{p}_T]. \tag{2}$$

A total of $2 \times 10^4$ molecular configurations of the system are selected at regular time intervals from the (equilibrated) molecular dynamics trajectory generated with GROMACS and stored on disk for later analysis. This set of configurations is then considered for the computation of the surface tension using the test-area method. For this purpose, we make use of a Monte Carlo program developed in our group to obtain the phase diagram of water.[12–14,16,56,57] The program (initially designed for constant-pressure simulations) allows for changes in the shape of the simulation box[58,59] and can therefore be easily adapted to the requirements of the test-area simulation technique in the canonical ensemble with virtual changes in the shape of the simulation cell. The implementation of the method involves two independent perturbations: one in which the area of the interface $S = L_x L_y$ increases to $S + \Delta S$, with an associated decrease in $L_z$ so as to keep the total volume constant; and the other one, in which $S$ decreases to $S - \Delta S$ with an associated increase in $L_z$. If the changes in configurational energy of these perturbations are denoted by $\Delta U^+ = U(S + \Delta S) - U(S)$ and $\Delta U^- = U(S - \Delta S) - U(S)$, respectively, one can show (see Gloor *et al.*[42]) that the surface tension can be obtained from the expression

$$\gamma = \lim_{\Delta S \to 0} \frac{-kT}{2\Delta S}(\ln\langle \exp(-\Delta U^+/kT)\rangle - \ln\langle \exp(-\Delta U^-/kT)\rangle), \tag{3}$$

where $k$ is Boltzmann constant. Here, the angular brackets denote a canonical average over configurations ($2 \times 10^4$ in the present case) in the reference (unperturbed) state. When implementing the perturbation, the positions of the oxygen atoms are held fixed (in simulation box units), and the positional coordinates of the rest of the hydrogens are rescaled so as to satisfy the appropriate values of the bond lengths and bond angles of the model; there is no change in the molecular orientations associated with the perturbations. One should note that the reciprocal space vectors change as a consequence of the change in shape of the simulation cell, so they have to be recalculated after the virtual moves. In practice, we consider a value of $\Delta S/S = \pm 0.0005$ in Eq. (3) for the relative perturbation in the area of the interface. According to Gloor *et al.*, this value is appropriate for the computation of the surface tension of the vapor-liquid interface in Lennard-Jones systems.

In practice, three calculations of the total energy of the system are required per snapshot to compute the values of $\Delta U^+$ and $\Delta U^-$ appearing in Eq. (3). The corresponding Boltzmann factors are accumulated and the final averages over the set of $2 \times 10^4$ configurations are then used for the computation of the surface tension from Eq. (3). The LJ part of the interactions is truncated at 13 Å. For simplicity, we do not use a switching function between 12 and 13 Å as we did in the course of the molecular dynamics runs. Though the Hamiltonian is not strictly the same as the one used to generate the molecular dynamics trajectories, the difference is so small that no significant effects should be expected. Ewald sums are used to deal with the long-range Coulombic interactions.[45] Here, we implement the original Ewald sums technique rather than the PME method previously used in our molecular dynamics simulations. The Coulombic interactions are truncated in the real-space sum at 13 Å. A total of approximately 2500 vectors are used in reciprocal space (more reciprocal vectors are considered in the directions where the reciprocal vectors are closer). In practice, the computation of the surface tension is organized in four blocks, so that the standard deviation of the block averages provides an estimate of the uncertainty of our results.

The equilibrium density profile $\rho(z)$ is computed at each temperature by averaging the histogram of densities along $z$ over the set of $2 \times 10^4$ configurations previously generated from molecular dynamics. The width of the density histograms is typically of 1 Å. The density profile is fitted to a hyperbolic tangent function of the form

$$\rho(z) = \tfrac{1}{2}(\rho_l + \rho_v) - \tfrac{1}{2}(\rho_l - \rho_v)\tanh[(z - z_0)/d], \tag{4}$$

where $\rho_l$, $\rho_v$, $z_0$, and $d$ are adjustable parameters corresponding to the liquid and vapor densities at coexistence, the position of the Gibbs-dividing surface, and the thickness of the vapor-liquid interface, respectively. It is customary to report the thickness of the interface in terms of the "10-90" thickness ($t$), which is related to $d$ by $t = 2.197\,2d$. Considering the hyperbolic tangent approximation for the density profile, it can be shown that an estimate of the tail correction to the surface tension due to the truncation of the LJ interaction is given by[24,60]

$$\gamma_{\text{tail}} = 12\pi\epsilon\sigma^6(\rho_l - \rho_v)^2 \int_0^1 ds \int_{r_c}^{\infty} dr\, \coth(rs/d)(3s^3 - s)/r^3. \tag{5}$$

Before presenting our results, we would like to stress that the methodology used in this work has the following advantages. The use of GROMACS allows us to study relatively large systems (containing a total of 1024 molecules) with interactions truncated at a relatively large value of the cutoff (larger than four molecular diameters) for a relatively long span of time (1.5–2 ns). These requirements are essential to obtain reliable values of such a sensitive quantity as it is the surface tension. A typical simulation involves (approximately) five days of CPU time in a Opteron 2.4 GHz. We find that GROMACS is about four times faster than our Monte Carlo program, the reason being probably related with the use of optimized codes for the calculation of the Ewald sums

TABLE I. Vapor-liquid coexistence properties for the TIP4P, SPC, and SPC/E models of water as computed from direct simulations of the inhomogeneous systems considered in this work at different temperatures $T$. The densities of the liquid ($\rho_l$) and vapor ($\rho_v$) phases are given in $g/cm^3$; $p$ is the vapor pressure. Also included for comparison are results obtained from Gibbs-ensemble simulations by Lisal *et al.* (Ref. 61) (TIP4P model), and by Errington and Panagiotopoulos (Ref. 21) (SPC and SPC/E models). The coexistence data of Ref. 21 can be found in tabular form in the web page of A. Z. Panagiotopoulos (Ref. 73).

| Model | Technique | $T$/K | $p$/bar | $\rho_l$ | $\rho_g$ |
|---|---|---|---|---|---|
| TIP4P | Gibbs ensemble | 350 | 0.57 | 0.952 | 3.6E−4 |
| TIP4P | This work | 350 | 0.4 | 0.950 | 4E−4 |
| TIP4P | Gibbs ensemble | 400 | 3.54 | 0.900 | 2.1E−3 |
| TIP4P | This work | 400 | 3.2 | 0.896 | 2.1E−3 |
| TIP4P | Gibbs ensemble | 450 | 13.33 | 0.831 | 7.7E−3 |
| TIP4P | This work | 450 | 13.61 | 0.824 | 7.8E−3 |
| TIP4P | Gibbs ensemble | 500 | 38.29 | 0.739 | 2.4E−2 |
| TIP4P | This work | 500 | 39.0 | 0.727 | 3.1E−2 |
| SPC | Gibbs ensemble | 300 | ⋯ | 0.975 | 2.3E−5 |
| SPC | This work | 300 | −0.04 | 0.974 | 2.9E−5 |
| SPC/E | Gibbs ensemble | 300 | 0.01 | 1.005 | 7.4E−6 |
| SPC/E | This work | 300 | −0.14 | 0.994 | 1.4E−5 |
| SPC/E | Gibbs ensemble | 350 | 0.143 | 0.961 | 8.8E−5 |
| SPC/E | This work | 350 | 0.05 | 0.962 | 9.2E−5 |
| SPC/E | Gibbs ensemble | 450 | 5.32 | 0.864 | 2.71E−3 |
| SPC/E | This work | 450 | 5.1 | 0.860 | 3.1E−3 |
| SPC/E | Gibbs ensemble | 500 | 15.5 | 0.792 | 8.16E−3 |
| SPC/E | This work | 500 | 17.0 | 0.788 | 0.010 |
| SPC/E | Gibbs ensemble | 550 | 39.9 | 0.703 | 0.022 |
| SPC/E | This work | 550 | 42.29 | 0.694 | 0.028 |

in the molecular dynamics code. The implementation of the test-area technique in our Monte Carlo program is quite straightforward and, what is even more important, allows one to compute the surface tension from a different route using a completely independent code. This offers a good cross checking of the quality of the results.

## III. RESULTS

We have computed a number of coexistence properties from simulations of inhomogeneous vapor-liquid systems at different temperatures and for a number of models of water. The vapor ($\rho_v$) and liquid ($\rho_l$) densities at coexistence are obtained from the running average of the corresponding density profile. The vapor pressure ($p$) is also calculated considering that for the planar geometry used here, the normal component ($p_N$) of the pressure tensor is constant throughout the system and equal to the vapor pressure. Our results for the different models used in this work are included in Tables I and II. As a check of consistency we compare the coexistence properties obtained from our direct simulations with those obtained by other authors (we only consider data from authors that treat the long-range Coulombic interactions properly either by using Ewald sums or the reaction field technique). The values of the coexistence pressure obtained from our inhomogeneous simulations of the TIP4P model are in good agreement with the values reported by Lisal *et al.* from Gibbs ensemble simulations.[61] Our results are also consistent with the values reported by Boulougouris *et al.*[20] and Errington and Panagiotopoulos[21] for the SPC/E model. A similar conclusion holds after comparing our results for the vapor pressure with those obtained for the TIP4/2005, TIP4P/Ew, and TIP4P/Ice models.[16,62,63] The latter were obtained from Hamiltonian Gibbs-Duhem integration using the TIP4P model as the initial reference Hamiltonian of the integration. According to the results included in Tables I and II, the values of the coexistence densities obtained from the inhomogeneous simulations are slightly (but systematically) lower (by about 0.5%) than those obtained from Gibbs ensemble or Hamiltonian Gibbs-Duhem integration. Also, the values of the vapor pressures calculated here are found to be slightly higher than those reported in the literature, particularly at high temperature. These differences can be traced back to the tail correction of the LJ interactions beyond the cutoff distance. These corrections can be easily incorporated in simulations involving homogeneous phases without the presence of the interface, as is the case of simulations implemented using the Gibbs ensemble or the Gibbs-Duhem integration techniques. In contrast, it is not straightforward to estimate the tail correction in simulations of inhomogeneous systems,[24,42] so the results reported in Tables I and II correspond to truncated interactions with no long-range corrections. The large value of the cutoff distance used in this work ensures that the contribution to the coexistence properties due to the tail correction is small.

TABLE II. Vapor-liquid coexistence properties for the TIP4P/2005, TIP4P/Ew, and TIP4P/Ice models of water as computed from direct simulations of the inhomogeneous systems considered in this work at different temperatures $T$. The densities of the liquid ($\rho_l$) and vapor ($\rho_v$) phases are given in $g/cm^3$; $p$ is the vapor pressure. Also included for comparison are results obtained from the Gibbs-Duhem simulation technique (Ref. 18).

| Model | Technique | $T$/K | $p$/bar | $\rho_l$ | $\rho_g$ |
|---|---|---|---|---|---|
| TIP4P/2005 | Gibbs-Duhem | 350 | 0.131 | 0.971 | 0.000 08 |
| TIP4P/2005 | This work | 350 | −0.02 | 0.968 | 0.000 06 |
| TIP4P/2005 | Gibbs-Duhem | 450 | 4.46 | 0.883 | 0.0023 |
| TIP4P/2005 | This work | 450 | 4.5 | 0.880 | 0.0025 |
| TIP4P/2005 | Gibbs-Duhem | 550 | 38.01 | 0.741 | 0.021 |
| TIP4P/2005 | This work | 550 | 38.3 | 0.733 | 0.023 |
| TIP4P/Ew | Gibbs Duhem | 350 | 0.176 | 0.969 | 0.000 11 |
| TIP4P/Ew | This work | 350 | −0.03 | 0.964 | 0.000 11 |
| TIP4P/Ew | Gibbs Duhem | 450 | 5.47 | 0.871 | 2.94E−3 |
| TIP4P/Ew | This work | 450 | 5.64 | 0.866 | 3.15E−3 |
| TIP4P/Ew | Gibbs Duhem | 550 | 44.62 | 0.714 | 0.027 |
| TIP4P/Ew | This work | 550 | 44.6 | 0.701 | 0.028 |
| TIP4P/Ice | Gibbs-Duhem | 450 | 1.51 | 0.913 | 7.63E−4 |
| TIP4P/Ice | This work | 450 | 1.16 | 0.910 | 8.1E−4 |
| TIP4P/Ice | Gibbs-Duhem | 550 | 16.32 | 0.811 | 0.0078 |
| TIP4P/Ice | This work | 550 | 15.7 | 0.807 | 0.0082 |
| TIP4P/Ice | Gibbs-Duhem | 600 | 40.0 | 0.740 | 0.020 |
| TIP4P/Ice | This work | 600 | 38.6 | 0.734 | 0.021 |

One should note, however, that the direct coexistence technique has difficulties at low temperature, where the vapor density is so low that the evaporation of a molecule of water from the liquid film becomes a rare event. As a consequence, it is difficult to obtain accurate values of the den-

TABLE III. Values of the surface tension (in $mJ/m^2$) for the TIP3P, SPC, SPC/E, and TIP4P models of water at different temperatures $T$ as obtained from simulation. $\rho_l$ and $\rho_v$ are the densities of the liquid and vapor phases at coexistence in units of $g/cm^3$. $\bar{p}_N$ and $\bar{p}_T$ are the macroscopic values of the normal and tangential components of the pressure tensor (in units of bar). $t$ is the thickness of the vapor-liquid interface (in units angstrom). $\gamma_v^*$ and $\gamma_{ta}^*$ are the values of the surface tension obtained from the virial route and the test-area method, respectively, without including long-range corrections; $\gamma_v$ and $\gamma_{ta}$ are the corresponding values of the surface tension, but including long-range corrections [see Eq. (5)]. The values of $r_c=13$ Å and $r_c=12.5$ Å were used to compute the tail corrections to $\gamma_{ta}^*$ and $\gamma_v^*$, respectively. The values of the surface tension as estimated from this work ($\gamma_{sim}$) correspond to the arithmetic average $(\gamma_v+\gamma_{ta})/2$. $\gamma_{exp}$ correspond to the experimental values of the surface tension.

| $T$/K | $\rho_l$ | $\rho_v$ | $\bar{p}_N$ | $\bar{p}_T$ | $\gamma_v^*$ | $\gamma_{ta}^*$ | $t$ | $\gamma_v$ | $\gamma_{ta}$ | $\gamma_{sim}$ | $\gamma_{exp}$ |
|---|---|---|---|---|---|---|---|---|---|---|---|
| TIP3P | | | | | | | | | | | |
| 300 | 0.980(2) | 0.000 024(5) | −0.11 | −98.44 | 49.2 | 49.8 | 3.87 | 52.4 | 52.2 | 52.3(1.5) | 71.73 |
| 450 | 0.790(1) | 0.0069(2) | 11.95 | −33.81 | 22.9 | 23.3 | 7.82 | 24.8 | 24.6 | 24.7(1.2) | 42.88 |
| SPC | | | | | | | | | | | |
| 300 | 0.974(2) | 0.000 029(2) | −0.04 | −103.10 | 51.5 | 52.1 | 3.75 | 54.9 | 54.6 | 54.7(1.7) | 71.73 |
| 450 | 0.805(1) | 0.0066(1) | 11.40 | −40.80 | 26.1 | 27.0 | 7.52 | 28.2 | 28.0 | 28.1(1.7) | 42.88 |
| SPC/E | | | | | | | | | | | |
| 300 | 0.994(2) | 0.000 014(2) | −0.14 | −120.50 | 60.2 | 60.8 | 3.39 | 63.7 | 63.5 | 63.6(1.5) | 71.73 |
| 350 | 0.962(1) | 0.0000 92(3) | 0.05 | −101.80 | 51.0 | 52.1 | 4.13 | 54.3 | 54.0 | 54.1(1.3) | 63.22 |
| 367 | 0.945(3) | 0.000 17(3) | 0.11 | −97.00 | 48.6 | 49.7 | 4.41 | 51.7 | 51.5 | 51.6(0.5) | 63.22 |
| 450 | 0.860(2) | 0.0031(2) | 5.10 | −63.60 | 34.3 | 35.0 | 6.22 | 36.8 | 36.6 | 36.7(1.0) | 42.88 |
| 500 | 0.788(2) | 0.010(2) | 17.00 | −31.00 | 24.0 | 24.3 | 8.09 | 26.0 | 25.8 | 25.9(1.5) | 31.61 |
| 550 | 0.694(2) | 0.028(2) | 42.30 | 17.20 | 12.5 | 13.1 | 11.40 | 13.8 | 13.7 | 13.8(1.2) | 19.69 |
| TIP4P | | | | | | | | | | | |
| 300 | 0.988(3) | 0.000 16(5) | −0.14 | −111.50 | 55.7 | 56.8 | 3.67 | 59.1 | 58.8 | 59.0(0.9) | 71.73 |
| 350 | 0.950(3) | 0.00 040(5) | 0.40 | −91.10 | 45.8 | 47.0 | 4.68 | 48.9 | 48.7 | 48.8(1.2) | 63.22 |
| 400 | 0.896(1) | 0.0021(1) | 3.20 | −68.80 | 36.0 | 36.8 | 5.69 | 38.7 | 38.5 | 38.6(1.5) | 53.33 |
| 450 | 0.825(1) | 0.0078(1) | 13.60 | −37.20 | 25.4 | 26.0 | 7.36 | 27.5 | 27.4 | 27.5(1.7) | 42.88 |
| 500 | 0.727(2) | 0.031(1) | 39.00 | 7.60 | 15.7 | 16.5 | 10.56 | 17.1 | 17.0 | 17.1(1.1) | 31.61 |

sity of the vapor phase in the low-temperature region unless very long runs are performed. Similarly, the values of the vapor pressure cannot be obtained with a high degree of accuracy in this region. Recall that the vapor pressure is just given by the normal component of the pressure tensor, $p_N$. However, much of the contribution to $p_N$ arises from the liquid side of the interface, where the uncertainty in the pressure for a run of about 2 ns is typically of 0.5 bar. Direct simulation of the inhomogeneous system is not a suitable technique for the determination of vapor pressures of water when the vapor pressure is smaller than, approximately, 0.5 bar. As a rule of thumb, one may conclude that the direct simulation technique can be used with confidence when the vapor pressure is not too small and the system is not too close to the critical temperature (say at least 90 K below). In spite of all the above comments, we may safely state that the direct simulation method employed here with parameters as described in this work yields coexistence densities and vapor pressures in good agreement with the results obtained from the Gibbs ensemble and/or the Gibbs-Duhem technique. This is reassuring, as one might expect a good description of the coexistence properties to be a prerequisite condition to a reliable description of the surface tension. Similar conclusions were obtained by Lopez-Lemus *et al.* for other type of molecules, such as *n*-alkanes.[64]

The values of the surface tension as obtained from the virial route ($\gamma_v$) and the test-area method ($\gamma_{ta}$) are reported in Tables III and IV. Results are presented for the TIP3P, SPC, SPC/E, and TIP4P (Table III) and for TIP4P/2005, TIP4P/Ew, and TIP4P/Ice (Table IV). We also include in these tables values of the vapor and liquid densities at coexistence, (macroscopic) components of the pressure tensor, and the 10-90 surface thickness, $t$. As explained in the previous section, the uncertainty in the values of the surface tension as obtained from the test-area method is estimated from the standard deviation of the corresponding block averages. Typically, the statistical errors are found to be of the order of 1 $mJ/m^2$. Uncertainties in the values of the surface tension obtained from the mechanical route depend on the errors associated with the components of the pressure tensor. Errors in $p_N$ and $p_T$ are of the order of 1 bar. This follows from the fact that the difference $p_{xx}-p_{yy}$ is always found to be zero within 1 bar in our simulations (here, $p_{xx}$ and $p_{yy}$ are Cartesian components of the pressure tensor; for the planar geometry considered here, it follows that $p_{xx}=p_{yy}=p_T$). Also, the running averages of the off-diagonal components of the pressure tensor are found to be zero within 1 bar. This yields an estimate of about 1 $mJ/m^2$ for the absolute error of the values of the surface tension obtained from the mechanical route. We thus find that both routes yield values of the surface tension of comparable accuracy. In addition, both routes yield consistent average values of the surface tension at all temperatures and for all models. According to our results, we find $\gamma_v$ to be essentially equal to $\gamma_{ta}$ within statistical uncertainties. Small differences between the values of $\gamma_v$ and $\gamma_{ta}$ can be observed, but they are simply due to the slightly different Hamiltonian used in the molecular dynamics and Monte Carlo programs, and to the slightly different treatment of the long-range Coulombic interactions in both programs. The tail correction to the surface tension is estimated from

TABLE IV. The same as Table III, but for the TIP4P/2005, TIP4P/Ew, and TIP4P/Ice models of water.

| $T$/K | $\rho_l$ | $\rho_v$ | $\bar{p}_N$ | $\bar{p}_T$ | $\gamma_v^*$ | $\gamma_{ta}^*$ | $t$ | $\gamma_v$ | $\gamma_{ta}$ | $\gamma_{sim}$ | $\gamma_{exp}$ |
|---|---|---|---|---|---|---|---|---|---|---|---|
| TIP4P/2005 | | | | | | | | | | | |
| 300 | 0.993(3) | 0.000010(3) | −0.09 | −130.60 | 65.3 | 65.5 | 3.22 | 69.5 | 69.1 | 69.3(0.9) | 71.73 |
| 350 | 0.968(2) | 0.000060(3) | −0.02 | −116.30 | 58.1 | 58.2 | 3.95 | 62.0 | 61.7 | 61.9(1.3) | 63.22 |
| 400 | 0.931(1) | 0.00060(3) | 0.60 | −97.20 | 48.9 | 49.3 | 4.73 | 52.5 | 52.2 | 52.3(1.4) | 53.33 |
| 450 | 0.880(1) | 0.0025(2) | 4.50 | −73.00 | 38.8 | 39.6 | 5.89 | 41.9 | 41.7 | 41.8(1.3) | 42.88 |
| 500 | 0.816(2) | 0.0073(3) | 13.70 | −43.20 | 28.5 | 28.4 | 7.48 | 31.0 | 30.8 | 30.9(0.8) | 31.61 |
| 550 | 0.733(1) | 0.023(1) | 38.30 | 3.40 | 17.4 | 17.3 | 9.90 | 19.2 | 19.1 | 19.2(1.0) | 19.69 |
| TIP4P/Ew | | | | | | | | | | | |
| 300 | 0.992(1) | 0.00000 | −0.10 | −123.60 | 61.7 | 62.4 | 3.34 | 65.4 | 65.1 | 65.2(1.1) | 71.73 |
| 350 | 0.964(2) | 0.00011(1) | −0.03 | −107.60 | 53.8 | 54.5 | 4.07 | 57.2 | 57.0 | 57.1(1.9) | 63.22 |
| 400 | 0.922(2) | 0.00068(8) | 0.90 | −88.10 | 44.5 | 45.5 | 4.95 | 47.6 | 47.4 | 47.5(1.5) | 53.33 |
| 450 | 0.866(1) | 0.0032(1) | 5.60 | −64.10 | 34.8 | 35.6 | 6.17 | 37.4 | 37.2 | 37.3(1.6) | 42.88 |
| 500 | 0.796(1) | 0.0098(3) | 17.30 | −30.90 | 24.1 | 24.1 | 8.06 | 26.2 | 26.0 | 26.1(0.6) | 31.61 |
| 550 | 0.701(2) | 0.028(1) | 44.60 | 16.80 | 13.9 | 14.0 | 11.12 | 15.3 | 15.2 | 15.3(1.0) | 19.69 |
| TIP4/Ice | | | | | | | | | | | |
| 300 | 0.990(3) | 0.000000 | −0.10 | −151.00 | 75.5 | 76.1 | 2.90 | 80.3 | 79.9 | 80.1(0.7) | 71.73 |
| 450 | 0.911(1) | 0.00083(5) | 1.20 | −103.80 | 52.5 | 52.8 | 4.94 | 56.4 | 56.1 | 56.3(1.3) | 42.88 |
| 550 | 0.807(1) | 0.0082(2) | 15.70 | −46.30 | 31.0 | 31.4 | 7.39 | 33.9 | 33.7 | 33.8(1.1) | 19.69 |
| 600 | 0.734(2) | 0.021(2) | 38.60 | −2.80 | 20.7 | 21.6 | 9.64 | 22.8 | 22.7 | 22.8(1.0) | 8.37 |

Eq. (5) using the appropriate value of the cutoff of the LJ interaction (notice the slightly different value of the truncation of the LJ interaction used in the molecular dynamics and in the Monte Carlo simulations). The final (and recommended) value of the surface tension $\gamma_{sim}$ are reported in Tables III and IV, and correspond to the average value of the surface tension as obtained from the virial and from the test area methods.

An important issue in simulations of inhomogeneous systems is whether the runs have been performed over a sufficiently long period of time. This is analyzed in Fig. 1, where we show the time dependence of the accumulated average values of the normal and tangential components of the pressure tensor for the TIP4P/2005 model at $T=300$ K. The accumulated values of the surface tension as obtained from the virial route (line) and from the test-area method (open circles) are also presented in the figure. According to the data included in Fig. 1, runs shorter than 0.5 ns are not sufficiently long so as to provide accurate values: a total simulation time of 1.5–2 ns, as we consider here, appears to be safe enough. A similar conclusion holds for all the simulations performed in this work. An inspection of Fig. 1 clearly indicates that the two routes used here for the calculation of the surface are fully consistent.

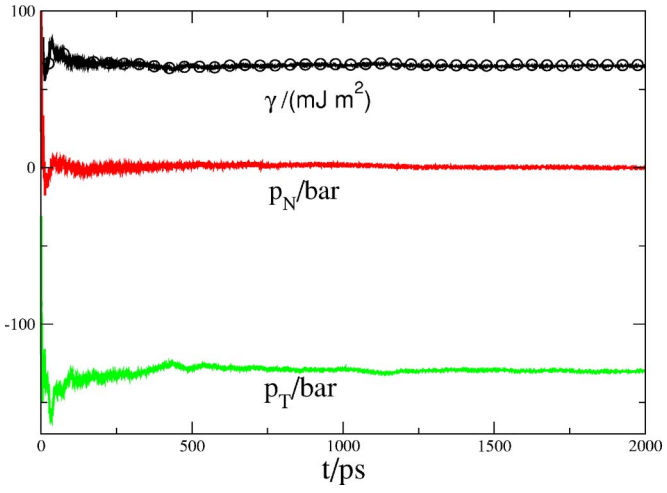


FIG. 1. Accumulated average values of the normal ($p_N$) and tangential ($p_T$) components of the pressure tensor as obtained from direct simulation of the vapor-liquid interface for the TIP4P/2005 model of water at a temperature of $T=300$ K. The accumulated average value of the surface tension as obtained from the pressure tensor with Eq. (2) is also presented (lines). The accumulated average values of the surface tension obtained from the test-area method with Eq. (3) are represented by the open circles.

In Fig. 2 we present the density profile $\rho(z)$ for the TIP4P/2005 model at $T=450$ K. The fact that the profile is essentially symmetric about the midpoint $z=L_z/2$ provides

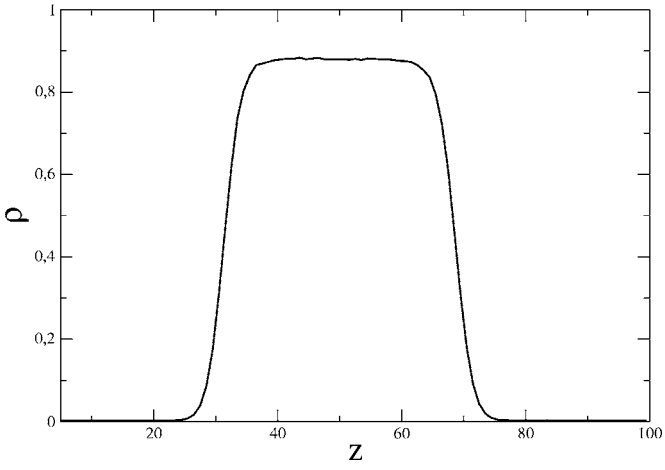


FIG. 2. The vapor-liquid density profile along the direction ($z$) normal to the interface as obtained from direct simulation of the inhomogeneous system for the TIP4P/2005 model of water at a temperature of $T=450$ K. The density $\rho$ is given in g/cm$^3$. The coordinate $z$ is given angstrom.

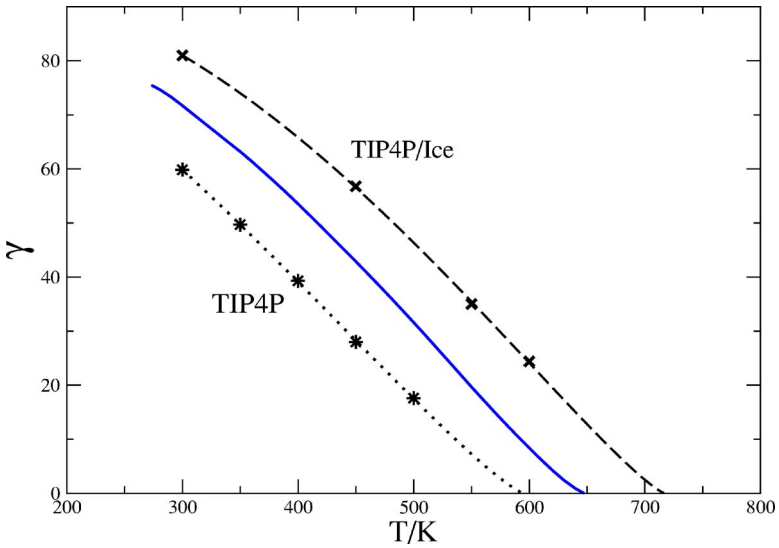


FIG. 3. Values of the surface tension of water as obtained from experiment (solid line), and from the computer simulations of this work for the TIP4P model (asterisks and dotted line), and for the TIP4P/Ice model (crosses and dashed line). The fits to the simulation results were obtained from Eq. (6). The surface tension is given in $mJ/m^2$.

additional evidence that the inhomogeneous system is properly equilibrated. The values of the 10-90 thickness ($t$) for the two interfaces shown in the figure are found to be 5.8 and 6.0 Å. The values of $t$ reported in Tables III and IV correspond to the average of the thickness of the right and left interfaces. These two values are never found to differ by more than 0.3 Å; this value provides an estimate of the uncertainty in the determination of this interfacial parameter. As can be seen in Fig. 2, the thickness of the liquid film along the $z$ direction is of about 30 Å, though the precise value depends on the model and also on the value of temperature.

We now proceed to compare the computed values of the surface tension from the different models of water ($\gamma_{sim}$) considered in this work with the corresponding experimental values. The values of $\gamma_{sim}$ for the TIP4P and TIP4P/Ice models are presented in Fig. 3. According to the data included in the figure, the TIP4P model yields values of the surface tension which are too low when compared with the experimental values. On the other hand, the TIP4P/Ice model clearly overestimates the interfacial tension. In Fig. 4 we present $\gamma_{sim}$ for the SPC/E and TIP4P/2005 models, whereas the results for the TIP4P/Ew are depicted in Fig. 5 and compared with those obtained for the TIP4P/2005 model. An inspection of Figs. 4 and 5 shows that the values of the surface tension of the SPC/E and TIP4P/Ew models are quite similar (see also the data included in Tables III and IV), though the latter are slightly higher. These two models provide values of $\gamma$ in much better agreement with experiments than the TIP3P, SPC, TIP4P, or TIP4P/Ice models. From the data shown in Figs. 3–5, we conclude that the best values of the surface tension of water are provided by the TIP4P/2005 model: the agreement with the experimental values is found to be quite satisfactory over the whole range of temperature from the triple point to the critical temperature. We recall at this point that the TIP4P/2005 model gives by far a better description of the liquid branch of the vapor-liquid equilibrium of water than any of the other model potentials considered here. It seems plausible to conclude that a quantitative description of the surface tension can only be achieved for models that yield correct liquid densities. We note that the TIP4P/2005 model also gives good estimates of the melting point and the critical temperature: the values 252 and 640 K, respectively, obtained from simulation are to be compared with the experi-

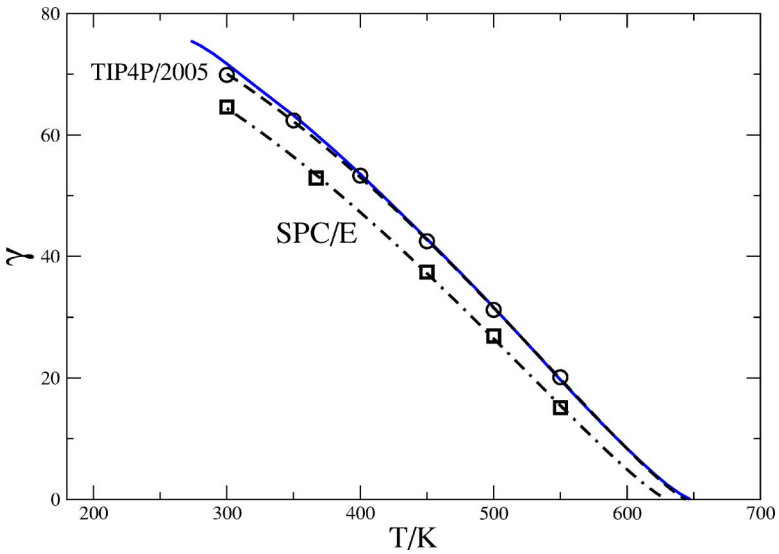


FIG. 4. Values of the surface tension of water as obtained from experiment (solid line), and from the computer simulations of this work for the SPC/E model (open squares and dashed-dotted line), and for the TIP4P/2005 model (open circles and dashed line). The fits to the simulation results were obtained from Eq. (6). The surface tension is given in $mJ/m^2$.

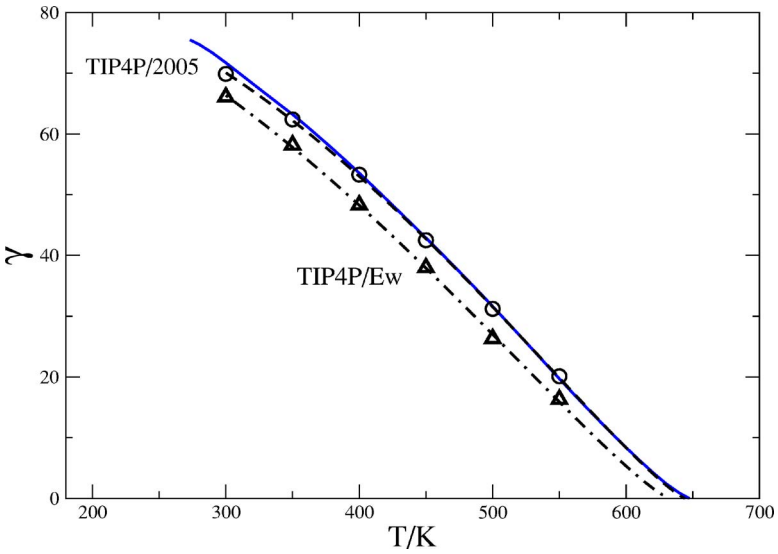


FIG. 5. Values of the surface tension of water as obtained from experiment (solid line), and from the computer simulations of this work for the TIP4P/Ew model (open triangles and dashed-dotted line), and for the TIP4P/2005 model (open circles and dashed line). The fits to the simulation results were obtained from Eq. (6). The surface tension is given in $mJ/m^2$.

mental values of 273 and 646 K. We also point out that by design, the SPC/E, TIP4P/Ew, and TIP4P/2005 models do not reproduce the experimental values of the vaporization enthalpy of water; these models can only reproduce the experimental value of the vaporization enthalpy when the polarization energy[7] is explicitly included. It thus follows that models which include such a term to reproduce the experimental values of the vaporization enthalpy of water are able to provide a reasonable description of the surface tension of water. As for the prediction of the critical temperature and orthobaric densities, these models are known to perform much better than models that do not include such a polarization term (TIP3P, TIP4P, SPC, TIP5P).

For each model, the following expression[65]

$$\gamma = c_1(1 - T/T_c)^{11/9}[1 - c_2(1 - T/T_c)] \quad (6)$$

is used to correlate the simulation data. This expression is used by the International Association for Properties of Water and Steam to describe the experimental values of the surface tension of water.[66,67] We shall also use it here to describe the surface tension of the different models of water. The expression contains three parameters to be determined, namely, $c_1$, $c_2$, and $T_c$. For $c_2=0$, the above expression reduces to the well-known Guggenheim[39,68] corresponding-states law. The value 11/9 for the exponent in Eq. (6) was first proposed by Guggenheim.[68] In addition to $c_1$ and $c_2$, we consider here $T_c$ as a free parameter to be obtained from the optimal fit to the surface tension data. The values of the fitting coefficients are reported in Table V for the SPC/E, TIP4P, TIP4P/2005, TIP4P/Ew, and TIP4P/Ice models; the corresponding continuous $\gamma(T)$ curves have been included in Figs. 3–5. We find that Eq. (6) describes quite accurately the variation of the surface tension with temperature for all models of water. A comparison of the values of $T_c$ obtained from the fit of the surface tension data with the critical temperatures obtained from independent sources is shown in Table V. An inspection of the values included in Table V shows that the agreement is quite satisfactory. In fact, as it can be seen our estimate of the critical temperature (from surface tension calculations) differ by about 5–10 K from that obtained from Gibbs ensemble simulations by other authors. The error in our estimate of $T_c$ due to the uncertities in the values of the surface tension is of about 4 K. As no many data points are used for each of the fits, one could argue that our numerical procedure to estimate the critical temperature is not fully justified. However, when the *experimental* values of the surface tension at temperatures $T/K=300$, 350, 400, 450, 500, and 550 are fitted to Eq. (6), one obtains an estimate of 644 K for the critical temperature, a value just 3 K below the experimental value of $T_c=647$ K. In sumary, when surface tensions are computed up to a temperature about 90 K below the critical temperature (including the tail correction to the surface tension due to the truncation of the LJ potential), and Eq. (6) is used to fit the results, then, good estimates of the critical temperature of the model are obtained. Notice, however, that the true critical point of a model where the LJ potential is truncated at about 13 Å would be slightly lower than the values reported in Table V.

It is interesting to note that all models of water are able to reproduce the weak *s* shape of the surface tension-temperature curve found experimentally for water, with a change in curvature as the system approaches the critical point. This behavior, which is not exhibited by nonassociat-

TABLE V. Fitting parameters [see Eq. (6)] to the values of the surface tension $\gamma_{sim}$ as obtained from simulations for different models of water. $c_1$ is given in $mJ/m^2$; $c_2$ is dimensionless, and $T_c$ is the critical temperature (in kelvin) resulting from the fit of Eq. (6). The last column includes the values of the critical temperature $T_c^*$ (in units of kelvin) as obtained from Gibbs-ensemble or Gibbs-Duhem simulations by Lisal *et al.* (Ref. 61) (TIP4P); Boulougouris *et al.* (Ref. 20), and Errington and Panagiotopoulos (Ref. 21) (SPC/E); and Vega *et al.* (Ref. 18) (TIP4P/2005, TIP4P/Ew, and TIP4P/Ice).

| Model | $c_1$ | $c_2$ | $T_c$ | $T_c^*$ |
|---|---|---|---|---|
| SPC/E | 205.32 | 0.6132 | 625.7 | 630 639 |
| TIP4P | 172.90 | 0.3929 | 593.9 | 588 |
| TIP4P/2005 | 227.86 | 0.6413 | 641.4 | 640 |
| TIP4P/Ew | 208.37 | 0.5878 | 628.3 | 628 |
| TIP4P/Ice | 256.24 | 0.6684 | 704.7 | 705 |

ing fluids, has been ascribed to hydrogen bonding,[39] and has been reproduced within a density-functional theory for associating fluids.[69,70]

## IV. CONCLUSIONS

We have computed the surface tension from direct simulation of the vapor-liquid interface for several models of water in a broad range of temperature. The total number of particles (1024), length of the simulations (2 ns), and cutoff distance of the interactions (13 Å) are chosen such that a confident computation of the surface tension is ensured. The values of coexistence properties, such as vapor and liquid densities and vapor pressures, obtained from simulations of the inhomogeneous system have been found to be in good agreement with those obtained from indirect simulation techniques, such as the Gibbs ensemble or Gibbs-Duhem integration. Vrabec *et al.*[40] have arrived to a similar conclusion in a recent study of the Lennard-Jones fluid. Small differences, however, have been found in the case of water and have been attributed to the difficulty in estimating the long-range contribution to the coexistence properties due to the truncation of the interactions in simulations of inhomogeneous systems.

The surface tension has been obtained from two different routes using, in each case, a different computer code and simulation technique. On the one hand, we have used a mechanical (virial) route and calculated the surface tension from the components of the pressure tensor obtained along the molecular dynamics trajectory generated using GROMACS (version 3.3). On the other hand, we have invoked a thermodynamic route and determined the interfacial tension from the average of the Boltzmann factor associated with perturbations of the area of the interface at constant volume. We have shown that the virial and area-perturbation routes for calculating the surface tension are consistent. Though both methods are fully equivalent, the test-area method has an apparent advantage over the virial route in that only energy calculations are required rather than evaluation of the forces (pair virials). The method is thus particularly well suited when Monte Carlo is the simulation technique of choice. We also recall that the evaluation of the pressure tensor for molecular fluids can be tricky, particularly in the case of molecules subject to geometrical constraints, as pointed out by Duque and Vega.[71] Obviously, the test-area method can be easily incorporated into a molecular dynamics simulation program or, as is done here, used for analyzing a set of trajectories generated from molecular dynamics. As for the estimates of the errors in the computed averages, both methods appear to provide a similar level of accuracy for all models of water at all the values of temperature considered here.

The computed values of the surface tension (with the corresponding tail correction being included) have been fitted to an empirical expression of the type proposed by Guggenheim,[68] from which estimates of the critical temperatures have been obtained for the different models of water considered in this work. The values of $T_c$ have been found to be in excellent agreement with values of the critical temperature reported in the literature obtained from extrapolation of the coexistence vapor-liquid densities as computed from Gibbs ensemble simulations for the same models. A comparison with experimental data has allowed us to assess the adequacy of each of the models considered here to reproduce the observed behavior of the surface tension of water. According to our results, models (such as SPC, TIP3P, and TIP4P) that reproduce the vaporization enthalpy of water yield too low values of the surface tension. On the other hand, the TIP4P/Ice model overestimates the surface tension (as it does for the vaporization enthalpy) at all temperatures. Much better agreement with experiments is provided by the SPC/E, TIP4P/Ew, and TIP4P/2005 models. These models reproduce the vaporization enthalpy of water only when the "polarization term" is explicitly included. The consideration of this term was first suggested by Berendsen *et al.*[7] for the SPC/E model. This polarization energy can also be used for TIP4P models. In fact, TIP4P/Ew and TIP4P/2005 are just the SPC/E-like variants of the original TIP4P model. These three models (SPC/E, TIP4P/Ew, and TIP4P/2005) give an improved description of the vapor-liquid equilibria of water: this seems to be a necessary condition for the appropriate description of the behavior of the surface tension. The TIP4P/2005 model is known to give a satisfactory description of the phase diagram of water, densities of the solid polymorphs, vapor-liquid equilibria, temperature of maximum density, diffusion coefficient, compressibility, thermal expansion coefficient, and structure. The model has also been successful in describing, for the first time, the chemical potential of methane in water, and the equation of state of the methane hydrate in a broad range of temperatures.[72] According to this work, a good description of the surface tension should be added to the merits of this model. It is fair to say, however, that the TIP4P/2005 model yields a poor description of the vapor phase (which seems unavoidable with nonpolarizable models), and a somewhat low dielectric constant, which seems to be also a common feature of TIP4P geometries.

## ACKNOWLEDGMENTS

This work has been supported by Project Nos. FIS2004-06227-C02-01 and FIS2004-06227-C02-02 from the Dirección General de Investigación and by Project No. S-0505/ESP/0299 from the Comunidad de Madrid. Further financial support from Junta de Andalucía and from the University of Huelva is gratefully acknowledged.

[1] J. A. Barker and R. O. Watts, Chem. Phys. Lett. **3**, 144 (1969).
[2] A. Rahman and F. H. Stillinger, J. Chem. Phys. **55**, 3336 (1971).
[3] B. Guillot, J. Mol. Liq. **101**, 219 (2002).
[4] W. L. Jorgensen and J. Tirado-Rives, Proc. Am. Acad. Arts Sci. **102**, 6665 (2005).
[5] W. L. Jorgensen, J. Chandrasekhar, J. D. Madura, R. W. Impey, and M. L. Klein, J. Chem. Phys. **79**, 926 (1983).
[6] H. J. C. Berendsen, J. P. M. Postma, W. F. van Gunsteren, and J. Hermans, in *Intermolecular Forces*, edited by B. Pullman (Reidel, Dordrecht, 1982), p. 331.
[7] H. J. C. Berendsen, J. R. Grigera, and T. P. Straatsma, J. Phys. Chem. **91**, 6269 (1987).
[8] M. W. Mahoney and W. L. Jorgensen, J. Chem. Phys. **112**, 8910 (2000).
[9] U. Essmann, L. Perera, M. L. Berkowitz, T. Darden, H. Lee, and L. G. Pedersen, J. Chem. Phys. **103**, 8577 (1995).
[10] H. W. Horn, W. C. Swope, J. W. Pitera, J. D. Madura, T. J. Dick, G. L. Hura, and T. Head-Gordon, J. Chem. Phys. **120**, 9665 (2004).

[11] J. L. F. Abascal and C. Vega, J. Chem. Phys. **123**, 234505 (2005).
[12] E. Sanz, C. Vega, J. L. F. Abascal, and L. G. MacDowell, Phys. Rev. Lett. **92**, 255701 (2004).
[13] E. Sanz, C. Vega, J. L. F. Abascal, and L. G. MacDowell, J. Chem. Phys. **121**, 1165 (2004).
[14] C. Vega, C. McBride, E. Sanz, and J. L. Abascal, Phys. Chem. Chem. Phys. **7**, 1450 (2005).
[15] C. Vega, J. L. F. Abascal, E. Sanz, L. G. MacDowell, and C. McBride, J. Phys.: Condens. Matter **17**, S3283 (2005).
[16] C. Vega, E. Sanz, and J. L. F. Abascal, J. Chem. Phys. **122**, 114507 (2005).
[17] R. G. Fernandez, J. L. F. Abascal, and C. Vega, J. Chem. Phys. **124**, 144506 (2006).
[18] C. Vega, J. L. F. Abascal, and I. Nezbeda, J. Chem. Phys. **125**, 034503 (2006).
[19] A. Baranyai, A. Bartok, and A. A. Chialvo, J. Chem. Phys. **124**, 074507 (2006).
[20] G. C. Boulougouris, I. G. Economou, and D. N. Theodorou, J. Phys. Chem. B **102**, 1029 (1998).
[21] J. R. Errington and A. Z. Panagiotopoulos, J. Phys. Chem. B **102**, 7470 (1998).
[22] M. Matsumoto, Y. Takaoka, and Y. Kataoka, J. Chem. Phys. **98**, 1464 (1993).
[23] K. Yasuoka and M. Matsumoto, J. Chem. Phys. **109**, 8463 (1998).
[24] J. Alejandre, D. Tildesley, and G. A. Chapela, J. Chem. Phys. **102**, 4574 (1995).
[25] R. S. Taylor, L. X. Dang, and B. C. Garrett, J. Phys. Chem. **100**, 11720 (1996).
[26] S. E. Feller, R. W. Pastor, A. Rojnuckarin, S. Bogusz, and B. R. Brooks, J. Phys. Chem. **100**, 17011 (1996).
[27] D. M. Huang, P. L. Geissler, and D. Chandler, J. Phys. Chem. B **105**, 6704 (1998).
[28] J. L. Rivera, M. Predota, A. A. Chialvo, and P. T. Cummings, Chem. Phys. Lett. **357**, 189 (2002).
[29] A. Wynveen and F. Bresme, J. Chem. Phys. **124**, 104502 (2006).
[30] A. E. Ismail, G. S. Grest, and M. J. Stevens, J. Chem. Phys. **125**, 014702 (2006).
[31] Y. J. Lu and B. Wei, Appl. Phys. Lett. **89**, 164106 (2006).
[32] B. Shi, S. Sinha, and V. K. Dhir, J. Chem. Phys. **124**, 204715 (2006).
[33] V. V. Zakharov, E. N. Brodskaya, and A. Laaksonen, J. Chem. Phys. **107**, 10675 (1997).
[34] B. B. Garret and G. K. Schenter, Chem. Rev. (Washington, D.C.) **106**, 1355 (2006).
[35] I. F. W. Kuo, C. J. Mundy, B. L. Eggimann, M. J. McGrath, J. I. Siepmann, B. Chen, J. Vieceli, and D. J. Tobias, J. Phys. Chem. B **110**, 3738 (2006).
[36] E. Chacon, P. Tarazona, and J. Alejandre, J. Chem. Phys. **125**, 014709 (2006).
[37] J. L. Rivera, F. W. Starr, P. Paricaud, and P. T. Cummings, J. Chem. Phys. **125**, 094712 (2006).
[38] J. L. Rivera, M. Predota, A. A. Chialvo, and P. T. Cummings, Chem. Phys. Lett. **357**, 189 (2002).
[39] J. S. Rowlinson and B. Widom, *Molecular Theory of Capillarity* (Clarendon, Oxford, 1982).
[40] J. Vrabec, G. K. Kedia, G. Fuchs, and H. Hasse, Mol. Phys. **104**, 1509 (2006).
[41] A. Trokhymchuk and J. Alejandre, J. Chem. Phys. **111**, 8510 (1999).
[42] G. J. Gloor, G. Jackson, F. J. Blas, and E. de Miguel, J. Chem. Phys. **123**, 134703 (2005).
[43] B. Widom, J. Chem. Phys. **39**, 2808 (1963).
[44] M. P. Allen and D. J. Tildesley, *Computer Simulation of Liquids* (Oxford University Press, New York, 1987).
[45] D. Frenkel and B. Smit, *Understanding Molecular Simulation* (Academic, London, 1996).
[46] V. I. Harismiadis, J. Vorholz, and A. Z. Panagiotopoulos, J. Chem. Phys. **105**, 8469 (1996).
[47] H. L. Vortler and W. R. Smith, J. Chem. Phys. **112**, 5168 (2000).
[48] E. de Miguel and G. Jackson, J. Chem. Phys. **125**, 164109 (2006).
[49] E. de Miguel and G. Jackson, Mol. Phys. **104**, 3717 (2006).
[50] D. V. der Spoel, E. Lindahl, B. Hess, G. Groenhof, A. E. Mark, and H. J. C. Berendsen, J. Comput. Chem. **26**, 1701 (2005).
[51] S. Nosé, Mol. Phys. **52**, 255 (1984).
[52] W. G. Hoover, Phys. Rev. A **31**, 1695 (1985).
[53] J. P. Ryckaert, G. Ciccotti, and H. J. C. Berendsen, J. Comput. Phys. **23**, 327 (1977).
[54] H. J. C. Berendsen and W. F. van Gusteren, *Molecular Liquids-Dynamics and Interactions* Proceedings of the NATO Advanced Study Institute on Molecular Liquids (Reidel, Dordretch, 1984), pp. 475–500.
[55] K. A. Feenstra, B. Hess, and H. J. C. Berendsen, J. Comput. Chem. **20**, 786 (1999).
[56] L. G. MacDowell, E. Sanz, C. Vega, and L. F. Abascal, J. Chem. Phys. **121**, 10145 (2004).
[57] C. McBride, C. Vega, E. Sanz, L. G. MacDowell, and J. L. F. Abascal, Mol. Phys. **103**, 1 (2005).
[58] M. Parrinello and A. Rahman, J. Appl. Phys. **52**, 7182 (1981).
[59] S. Yashonath and C. N. R. Rao, Mol. Phys. **54**, 245 (1985).
[60] G. A. Chapela, G. Saville, S. M. Thompson, and J. S. Rowlinson, J. Chem. Soc., Faraday Trans. 2 **8**, 133 (1977).
[61] M. Lisal, W. R. Smith, and I. Nezbeda, Fluid Phase Equilib. **181**, 127 (2001).
[62] D. A. Kofke, J. Chem. Phys. **98**, 4149 (1993).
[63] R. Agrawal and D. A. Kofke, Mol. Phys. **85**, 23 (1995).
[64] J. Lopez-Lemus, M. Romero-Bastida, T. A. Darden, and J. Alejandre, Mol. Phys. **104**, 2413 (2006).
[65] *Water in Biology, Chemistry and Physics: Experimental Overviews and Computational Methodologies*, edited by G. W. Robinson, S. Singh, S. B. Zhu, and M. W. Evans (World Scientific, Singapore, 1996).
[66] M. Chaplin, http://www.lsbu.ac.uk/water/ (2005).
[67] H. J. White, J. V. Sengers, D. B. Neumann, and J. C. Bellows, IAPWS Release on the Surface Tension of Ordinary Water Substance (1995).
[68] E. A. Guggenheim, J. Chem. Phys. **13**, 253 (1945).
[69] F. J. Blas, E. M. del Rio, E. de Miguel, and G. Jackson, Mol. Phys. **99**, 1851 (2001).
[70] G. J. Gloor, F. J. Blas, E. M. del Rio, E. de Miguel, and G. Jackson, Fluid Phase Equilib. **194**, 521 (2002).
[71] D. Duque and L. F. Vega, J. Chem. Phys. **121**, 8611 (2004).
[72] H. Docherty, A. Galindo, C. Vega, and E. Sanz, J. Chem. Phys. **125**, 074510 (2006).
[73] http://kea.princeton.edu